Springer

Journal of Mechanical Science and Technology 23 (2009) 2747~2756

Journal of Mechanical Science and Technology

www.springerlink.com/content/1738-494x
DOI 10.1007/s12206-009-0810-9

Steering control algorithm for efficient drive of a mobile robot with steerable omni-directional wheels †

Jae-Bok Song[1,*] and Kyung-Seok Byun[2]

[1]*School of Mechanical Engineering, Korea University, Seoul, 136-713, Korea*
[2]*Department of Mechanical Engineering, Mokpo National University, Mokpo, 534-729, Korea*

(Manuscript Received July 28, 2008; Revised April 5, 2009; Accepted April 14, 2009)

Abstract

Omnidirectional mobile robots are capable of arbitrary motion in an arbitrary direction without changing the direction of wheels because they can perform 3-DOF motions on a plane. This paper presents a novel mobile robot design with steerable omnidirectional wheels. This robot can operate in either omnidirectional or differential drive modes, depending on the drive conditions. In the omnidirectional mode, the robot has 3 DOF in motion and 1 DOF in steering, which can function as a continuously variable transmission (CVT). The CVT function can be used to enhance the efficiency of the robot operation by increasing the range of the velocity ratio of the robot velocity to wheel velocity. The structure and kinematics of this robot are presented in detail. In the proposed steering control algorithm, the steering angle is controlled such that the motors may operate in the region of high velocity and low torque, thus operating with maximum efficiency. Various tests demonstrate that the motion control of the proposed robot works satisfactorily and the proposed steering control algorithm for CVT can provide a higher efficiency than the algorithm using a fixed steering angle. In addition, it is shown that the differential drive mode can give better efficiency than the omnidirectional-drive mode.

Keywords: Omnidirectional mobile robot; Steering control algorithm; Efficient drive; Continuously variable transmission (CVT)

1. Introduction

The applications of wheeled mobile robots have recently extended to service robots for the handicapped or the elderly and industrial mobile robots that operate in various environments. The most popular wheeled mobile robots are equipped with two independent driving wheels. Since these robots possess 2 DOF, they can rotate about any point, but cannot perform omnidirectional motion such as sideways motion. Omnidirectional mobile robots (OMRs) were proposed for overcoming such limitations. OMRs can be classified into the holonomic and non-holonomic types. Non-holonomic OMRs have limited motions; for example, they must steer the wheels before motion [1]. This paper describes holonomic OMRs. OMRs can move in an arbitrary direction without changing the direction of the wheels because they can achieve 3 DOF motions on a plane. Among the OMRs that have been proposed thus far, popular ones include universal wheel based robots [2] and, ball wheel based robots [3], and conventional-wheel robots [4].

OMRs using omnidirectional wheels comprising passive rollers or balls usually have three or four wheels. Three-wheeled OMRs are capable of achieving 3 DOF motions by driving three independent actuators [5, 6]; however, they may have stability problems due to the triangular contact area with the ground and the payload they carry, especially when

† This paper was recommended for publication in revised form by Associate Editor Doo Yong Lee
*Corresponding author. Tel.: +82 2 3290 3363, Fax.: +82 2 3290 3757
E-mail address: jbsong@korea.ac.kr

traveling on a ramp with a high center of gravity. Therefore, four-wheeled vehicles are preferred when stability is of great concern [7]. However, independent driving of four wheels creates one extra DOF. To deal with this redundancy problem, a mechanism that used three actuators to drive four omnidirectional wheels was suggested [8].

One approach to a redundant DOF is to devise some mechanism that uses this redundancy to change the wheel arrangement [9]; such a mechanism is called a variable footprint mechanism. Since the relationship between robot velocity and wheel velocities depends on the wheel arrangement, varying the wheel arrangement can function as a transmission. However, such mobile robots must limit their range of wheel arrangement to maintain the stability of the vehicle, which tends to lower the transmission performance. To overcome this limitation, the omnidirectional mobile robot with steerable omnidirectional wheels (OMR-SOW) was proposed, as shown in Fig. 1 [10]. Since the OMR-SOW significantly extended the range of the velocity ratio, stability was guaranteed irrespective of the wide range of wheel arrangements.

Efficiency is of great importance in mobile robots because it is directly related to the continuous operating time. Here efficiency implies the ratio of the mechanical energy generated by the motors to the electric energy supplied by the battery. If the robot requires less energy than another for performing the same motion, it is said to execute an efficient drive. In other words, a more efficient drive enables the robot to cover a longer distance for the same battery. The OMR-SOW acts as a continuously variable transmission (CVT) because the robot velocity can be changed continuously by adjusting the wheel arrangements without employing a gear train. The CVT can provide an efficient drive for OMR-SOW. If the CVT is not properly controlled, however, the efficiency can be deteriorated. Hence, a proper control algorithm is essential for an efficient drive. However, the CVT control of OMR-SOW is quite different from that of an automobile in that it is related to all four motors unlike an automotive CVT [9]. In this paper, a simple and effective steering algorithm that improves the motor drive efficiency through CVT control is suggested and verified by various experiments.

OMR-SOW has some drawbacks. When omnidirectional capabilities are not required in normal straight-line driving, the omnidirectional mechanism

Fig. 1. OMR-SOW.

tends to prevent the robot from driving efficiently. In this case, the wheel arrangement used in an automobile (i.e., four wheels in parallel) is preferred to the omnidirectional mechanism. Furthermore, the maximum height of a surmountable bump for OMR is limited by the radius of the passive roller of the omnidirectional wheel, which is much smaller than the radius of the wheel of an ordinary mobile robot. To overcome these drawbacks, the robot should function as an ordinary mobile robot unless its task requires omnidirectional capabilities. This paper proposes a new mechanism that can be used as a differential as well as an omnidirectional drive mechanism.

The remainder of this paper is organized as follows. Section 2 introduces the structure of the OMR-SOW and presents its kinematics. Section 3 explains the steering algorithm for the CVT proposed for an efficient drive of OMR-SOW. Section 4 provides some experimental results and investigates the validity of the proposed algorithm. Section 5 presents the conclusions.

2. Structure and operation of OMR-SOW

This section describes a new type of OMR, namely, an omnidirectional mobile robot with steerable omnidirectional wheels (OMR-SOW). Since the four wheels of this type of robot can be independently driven, OMR-SOW is a 4-DOF robot (i.e., 2 DOF are assigned for translation, 1 DOF for rotation and 1 DOF for steering). The steering DOF can function as a continuously variable transmission (CVT). In the following subsections, steerable omnidirectional wheels are described and the features of OMR-SOW are discussed in detail.

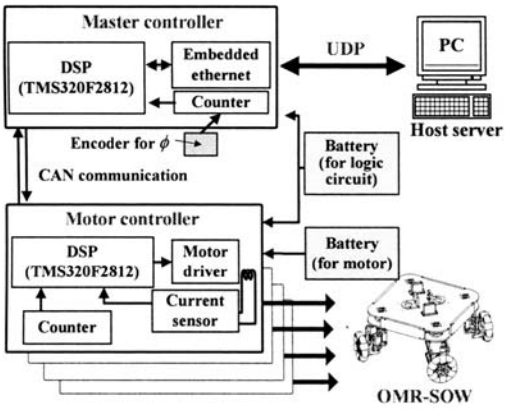

Fig. 2. Control systems for OMR-SOW.

2.1 Structure of OMR-SOW

In this paper the OMR-SOW developed in [10] was modified so that it could be operated in the differential drive mode by maintaining the steering angle at $\pm 45^{o}$ and preventing the passive rollers from rolling. This robot contains four wheel modules comprising an omnidirectional wheel connected to each motor, a synchronous steering mechanism, and a square platform with a side of 0.5m. The height of the platform from the ground is 0.42m. The robot can be used as a wheelchair since it was designed to carry a payload of more than 100kg. The drive mechanism uses four DC servo motors (150W) that are controlled by DSP-based motor controllers having a sampling period of 1 ms. The DSP-based master controller performs kinematic analysis, plans the robot trajectory, and delivers the velocity commands to each wheel. The robot can move autonomously, and the PC monitors the entire system, collects data, and displays the robot's states [10]. The suspension system, consisting of a four bar linkage, a damper and a spring, is required to ensure that all wheels are in contact with the ground at all times, which is very important in this type of four-wheeled mechanism. This suspension can also absorb the shocks transmitted to the wheels. Table 1 summarizes the specifications of the OMR-SOW.

The coordinate systems for OMR-SOW are shown in Fig. 3. The frame *O-XY* is assigned as the reference frame for robot motion in the plane, and the moving frame *o-xy* is attached to the robot center. The angle θ between the *y*-axis and the diagonal line of the robot body depends on the shape of the body (i.e., $\theta = 45^{o}$ for a square body). The four wheel modules can rotate about each pivot point C_1, .., C_4 located at the corners

Table 1. Specifications of OMR-SOW.

Features			Specifications
Robot	Weight		49.2 kg
	Width*Length*Height		0.7*0.7*0.42 m
	Battery	Logic circuit	12V, 7AH
		Motors	24V, 10AH
Wheel	Radius of wheel		0.10 m
	Radius of outer roller		0.0278 m
	Radius of inner roller		0.0209 m
Motor	Assigned power rating		150 W
	Nominal voltage		24 V
	Stall torque		2.29 Nm
	Max. continuous current		6.0 A
	Max. continuous torque		0.18 Nm

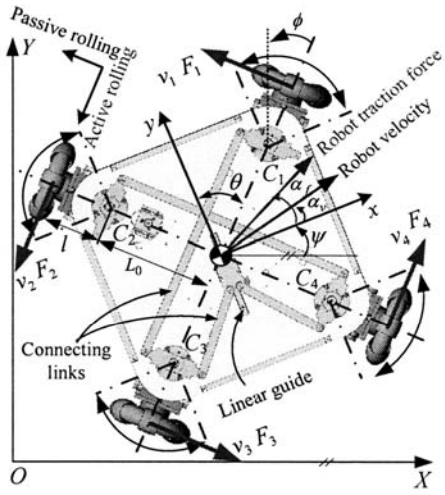

Fig. 3. Coordinate systems for OMR-SOW.

of the robot body, but they are constrained to execute a synchronized steering motion of a single DOF by the mechanism of connecting links and a linear guide. In Fig. 3, the steering angle ϕ is defined as the angle from the zero position that coincides with the diagonal lines (i.e., C_1C_3 or C_2C_4) of the robot body. Although four wheel modules are steered at each steering axis, the steering angle ϕ is identical for each wheel. Note that the steering is indirectly determined by the vector sum of each wheel velocity vector (not by an independent steering motor).

2.2 Omnidirectional wheels

Byun and Song [12] developed and patented the

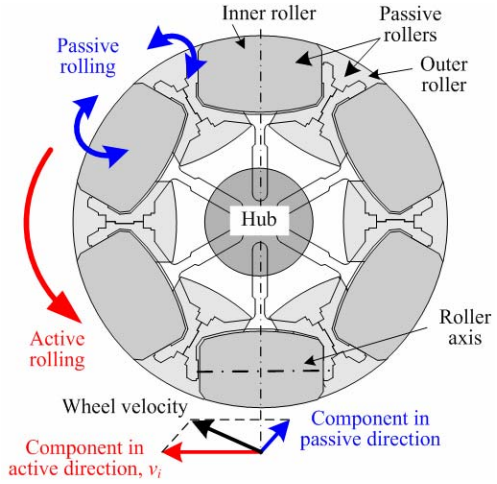

Fig. 4. CAW and active and passive rolling.

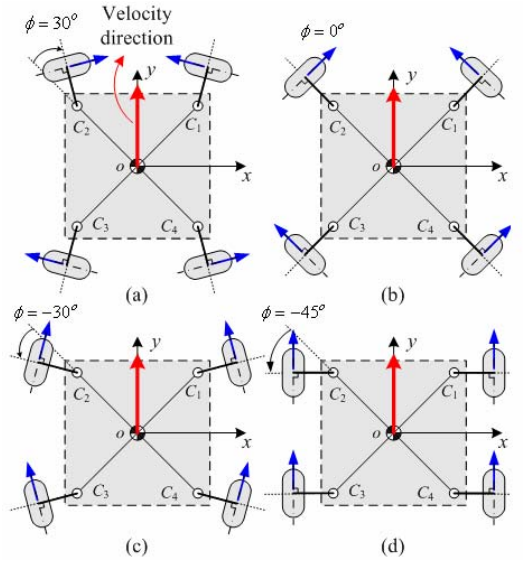

Fig. 5. Various wheel arrangements; (a) ϕ=30°, (b) ϕ=0°, (c) ϕ= - 30°, (d) ϕ= - 45° (differential drive).

omnidirectional wheels used in OMR-SOW, called *continuous alternate wheels* (CAW), where the inner and outer rollers are arranged continuously such that there are no gaps between the rollers, as shown in Fig. 4. Since the CAW makes continuous contact with the ground by alternating the large and small rollers around the wheel, virtually no vibrations are created during operation. In the CAW, the wheel velocity can be divided into the components along the active and passive directions, as shown in Fig. 4. The active component is directed along the axis of the roller in contact with the ground, while the passive one is perpendicular to the roller axis.

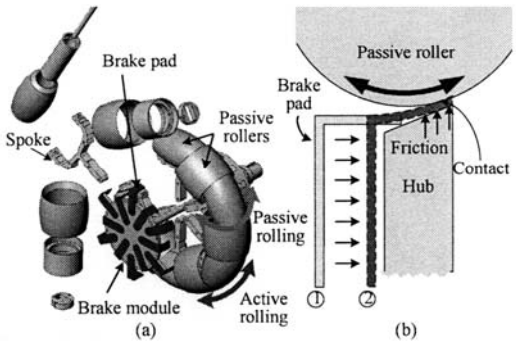

Fig. 6. (a) Disassembled CAW with brake module, and (b) passive roller brake mechanism.

The CAW developed in this paper can perform differential as well as omnidirectional drives: the steering angle is changed in the range of -30° to +30° in the omnidirectional drive mode, but maintained at +45° or -45° in the differential drive mode as shown in Fig. 5. The conventional wheels used in the differential drive have two advantages over omnidirectional wheels. First, the differential drive is generally more efficient than the omnidirectional drive when the latter is not required (e.g., straight-line driving). Second, the conventional wheels can go over a higher bump than the omnidirectional wheels because the maximum height of a surmountable bump for the omnidirectional wheels is limited by the radius of its passive roller, which is much smaller than the radius of a conventional wheel.

However, the differential drive mode cannot be set up by simply adjusting the steering angle of the omnidirectional wheels to +45° or - 45° because the passive rollers cannot be constrained in this case. For example, as shown in Fig. 5(d), pushing the robot along the x direction causes the robot to move in this direction, which does not happen in a robot with conventional wheels since such wheels resist sideways motion. In other words, passive rolling must not be allowed in the differential drive mode.

To overcome this problem, a passive roller brake mechanism was developed to stop the free rolling of the passive rollers in the differential drive mode, as shown in Fig. 6. This brake has 12 brake pads on its circumference. In the omnidirectional drive mode, the brake pads are placed in position 1, as shown in Fig. 6(b), so that they do not make contact with the passive rollers. However, in the differential drive mode, they are pulled toward the passive rollers (i.e., posi-

tion 2). The brakes pads are then elastically deformed and come in tight contact with the rollers such that they are locked.

2.3 Kinematic analysis

The relationship between the wheel velocity vector V_w and the robot velocity vector V_r is given by

$$V_w = J^{-1}V_r \quad \text{or} \quad V_r = JV_w \tag{1}$$

where $V_w = [v_1 \ v_2 \ v_3 \ v_4]^T$, $V_r = [v_x \ v_y \ \dot{\psi} \ \dot{\phi}]^T$, and the Jacobian matrix is given as

$$\mathbf{J} = \frac{1}{4}\begin{bmatrix} -1/C & -1/C & 1/C & 1/C \\ 1/S & -1/S & -1/S & 1/S \\ 1/L & 1/L & 1/L & 1/L \\ 1/l & -1/l & 1/l & -1/l \end{bmatrix}, \begin{cases} C = \cos(\theta - \phi) \\ S = \sin(\theta - \phi) \\ L = L_o \cos\phi + l \end{cases} \tag{2}$$

where v_1, v_2, v_3, and v_4 denote the velocities of the wheel centers along the active direction, v_x and v_y the translational velocities of the robot center, $\dot{\psi}$ the angular velocity of the robot body, and $\dot{\phi}$ the derivative of the steering angle, respectively. Further, l denotes the offset distance and L_0 the distance from the robot center to the steering axis, as shown in Fig. 3. It follows from Eq. (1) that the robot velocity and steering velocity of the OMR-SOW can be completely determined by the control of the four independent motors driving each wheel. Since the OMR is of 3 DOF in a plane, it is difficult to define the velocity ratio in terms of scalar velocities. Therefore, the velocity ratio is defined using the concept of norms as follows:

$$r_v = \frac{\| V_r^* \|}{\| V_w \|} = \frac{\| J^* V_w \|}{\| V_w \|}, \quad J^* = \frac{1}{4}\begin{bmatrix} -1/C & -1/C & 1/C & 1/C \\ 1/S & -1/S & -1/S & 1/S \\ L^*/L & L^*/L & L^*/L & L^*/L \\ l^*/l & -l^*/l & l^*/l & -l^*/l \end{bmatrix} \tag{3}$$

where $V_r^* = [v_x \ v_y \ L^*\dot{\psi} \ l^*\dot{\phi}]^T$ represents the normalized robot velocity, J^* is the normalized Jacobian, and L^* and l^* are the characteristic lengths for rotation and steering, respectively. These characteristic lengths are the design parameters used to normalize the Jacobian. Saha [13] selected a characteristic length to make the Jacobian matrix isotropic (i.e., to minimize the condition number), which was also adopted in the design of OMR-SOW. To make the Jacobian of the OMR-SOW isotropic, the elements of

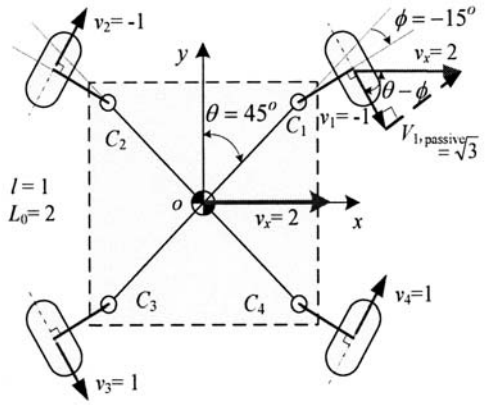

Fig. 7. Example in kinematics.

the normalized Jacobian must have the following relations:

$$\cos(\theta + \phi) = (L_0 \cos\phi + l)/L^* = l/l^* \tag{4}$$

Since the Jacobian of OMR-SOW is a function of the steering angle ϕ, Eq. (4) cannot hold for all ϕ. Therefore, the characteristics lengths are determined by assuming $\phi = 0$ in Eq. (4) as follows:

$$L^* = \sqrt{2}(L_0 \cos\phi + l), \ l^* = \sqrt{2}l \ , \tag{5}$$

When the value of ϕ is changes, the normalized Jacobian is not isotropic; however, the velocity ratio of Eq. (3) maintains dimensional homogeneity.

The operational principle of the OMR-SOW can be explained by considering the following example. Suppose $\theta = 45^o$, $\phi = -15^o$, $L_o = 2$, and $l = 1$, as shown in Fig. 7. If the robot velocity is given by $V_r = [2 \ \ 0 \ \ 0 \ \ 0]^T$, C, S and L become

$$\begin{aligned} C &= \cos(45^o + 15^o) = 0.5 \\ S &= \sin(45^o + 15^o) = 0.87 \\ L &= L_o \cos(-15^o) + l = 2.93 \end{aligned} \tag{6}$$

Then, Eq. (1) can be calculated as

$$\begin{Bmatrix} v_1 \\ v_2 \\ v_3 \\ v_4 \end{Bmatrix} = \begin{bmatrix} -0.5 & 0.87 & 2.93 & 1 \\ -0.5 & -0.87 & 2.93 & -1 \\ 0.5 & -0.87 & 2.93 & 1 \\ 0.5 & 0.87 & 2.93 & -1 \end{bmatrix} \begin{Bmatrix} 2 \\ 0 \\ 0 \\ 0 \end{Bmatrix} = \begin{Bmatrix} -1 \\ -1 \\ 1 \\ 1 \end{Bmatrix} \tag{7}$$

Fig. 7 shows the active wheel velocities required to

produce the desired robot velocity. Note that the desired robot velocity contains only the translational velocity along the x direction, so the resultant velocity of each wheel has a magnitude of 2 along the x direction. From this observation, it follows that the passive wheel velocity of wheel 1 has a magnitude of $\sqrt{3}$, which contributes to the specified resultant wheel velocity, as shown in Fig. 7.

On the other hand, the force and moment of a robot can be expressed by

$$F_r = J^{-T} F_w \quad \text{or} \quad F_w = J^T F_r \tag{8}$$

where $F_w = [F_1\ F_2\ F_3\ F_4]^T$ and $F_r = [F_x\ F_y\ T_z\ T_\phi]^T$. F_x and F_y denote the forces acting on the robot center along the x and y directions, T_z the moment about the z axis, and T_ϕ the torque required to rotate the wheel modules, respectively. The force F_i (i =1,.., 4) is the traction force acting on the wheel in the direction of active rolling as shown in Fig. 2. The force ratio of the force acting on the robot center to the wheel traction force can be defined in the same way as the velocity ratio in Eq. (3) as follows

$$r_f = \frac{\| F_r^* \|}{\| F_w \|} = \frac{\| J^{*-T} F_w \|}{\| F_w \|} \tag{9}$$

where F_r^* denotes the normalized robot traction force. Note that the force ratio corresponds to the inverse of the velocity ratio.

3. Steering control algorithm for CVT

In this section, a steering algorithm for CVT is discussed. The CVT of an automobile can keep the engine running within the optimal range with respect to fuel efficiency or performance. Using the engine efficiency data, the CVT controls the engine operating points under various vehicle conditions. A CVT control algorithm for OMR-SOW should consider the effects of all four motors. A simple and effective algorithm for control of the CVT is proposed based on the analysis of the operating points of a motor.

3.1 Motion control of OMR-SOW

The motion of a mobile robot can be controlled by wheel velocities. From Eq. (1), when the desired robot motion V_{rd} is given, the reference wheel velocity

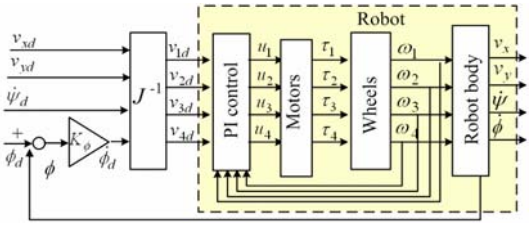

Fig. 8. Control system of OMR-SOW with steering angle control.

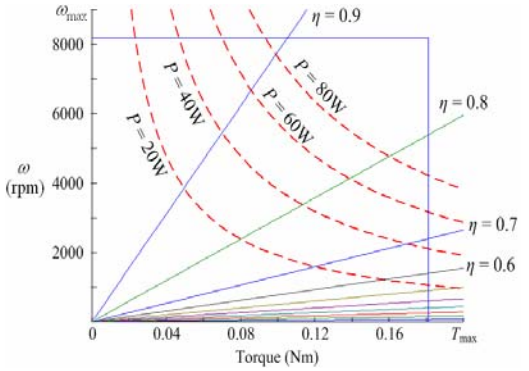

Fig. 9. Operating range of a motor.

V_{wd} of each wheel can be computed by

$$V_{wd} = J^{-1} V_{rd} \tag{10}$$

Fig. 8 shows the block diagram of the control system for OMR-SOW. When the reference wheel velocity $V_{wd} = [v_{1d}\ v_{2d}\ v_{3d}\ v_{4d}]^T$ is provided to each motor, the PI controller performs the velocity control of each motor to generate the control signal u_i (i = 1, .., 4). If each wheel is controlled to follow the reference wheel velocity, then the robot can achieve the desired motion. Practically, slips between the wheels and the ground occur to some extent in all mobile robots. Such slips cause the real motion to be different from the desired one. Since the robot does not have any sensor that measures the robot velocity, such errors are inevitable.

Since four wheels are independently controlled in OMR-SOW, a steering angle can be arbitrarily selected while the desired robot velocity (i.e., 2 translational DOF and 1 rotational DOF) is achieved. In other words, a wide range of steering angles can lead to an identical robot velocity. The steering control algorithm then determines the desired steering angle ϕ_d to achieve the maximum efficiency for the given

robot velocity. Therefore, the desired steering velocity is computed by

$$\dot{\phi}_d = K_\phi(\phi_d - \phi) \tag{11}$$

where K_ϕ denotes the control gain of steering and ϕ denotes the actual steering angle measured by the encoder installed on one of the steering axes (note that the steering angle is identical to all wheels).

Fig. 9 shows the operating points of the motor used in the mobile robot. In the figure, T_{max} represents the maximum continuous torque, and ω_{max} denotes the maximum permissible angular velocity. The solid and dashed lines represent the constant efficiency and the constant output power, respectively. The input power is obtained by the product of the input current and voltage, whereas the output power is measured by the product of the motor angular velocity and torque. The efficiency η is the ratio of the output power to the input power for a single motor.

As shown in this figure, the efficiency varies as the operating point moves on the constant output power line. The operating point of a motor can be varied by the CVT. For the same output power, a reduction in the force ratio of CVT leads to a decrease in velocity and an increase in torque, which in turn leads to a decrease in efficiency. Therefore, the CVT should be controlled such that motors operate in the region of high velocity and low torque.

3.2 Steering control algorithm

As explained in Section 3.1, when the desired robot velocity V_{rd} is given, each wheel is independently controlled. Any robot velocity can by achieved for a wide range of steering angles; nonetheless, some steering angles can provide a better efficiency than others. This section describes the proposed steering control algorithm that can determine a steering angle that results in maximum efficiency.

The velocity is controlled by each motor controller, as shown in Fig. 9. The current sensor at each motor drive measures the motor current and computes the motor torque $\tau = [\tau_1 \ \tau_2 \ \tau_3 \ \tau_4]^T$. The wheel traction force F_w can then be computed by

$$F_w = (\tau - I_w \dot{\omega}_w - c_w \omega_w)/r \tag{12}$$

where r denotes the wheel radius, I_w the moment of inertia of the wheel about the wheel axis, c_w the viscous friction factor of the wheel, and $\omega_w = [\omega_1 \ \omega_2 \ \omega_3 \ \omega_4]^T$ is the wheel angular velocity. By substituting (12) into (8), the robot traction force F_r can be obtained by

$$F_r = [F_x \ F_y \ T_z \ T_\phi]^T = J^{-T} F_w \tag{13}$$

In Eq. (13), the torque T_ϕ required to steer a wheel module is independent of the steering angles. Since the force ratio associated with rotation is hardly affected by the steering angles, it is mostly governed by translational motions [10]. The robot traction force direction α_f can then be given by

$$\alpha_f = \text{atan2}(F_x, F_y) \tag{14}$$

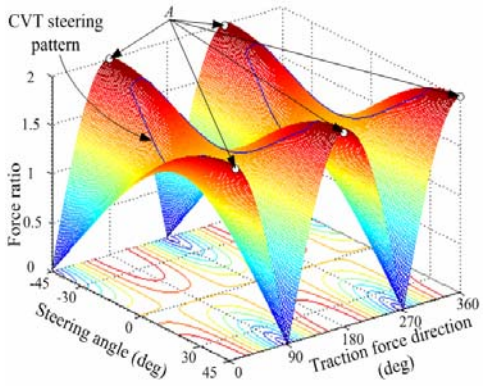

Fig. 10. Force ratio as a function of steering angle and force direction.

Fig. 10 shows the force ratio r_f defined in (9) in terms of the robot traction force angle α_f and the steering angle ϕ. Identical wheel traction forces can generate substantially different robot traction forces depending on ϕ. As explained in Section 3.1, the OMR-SOW capable of CVT has the maximum efficiency in the region with the highest force ratio (i.e., high velocity and low torque). For example, when $\alpha_f = 90^o$, a steering angle of -30^o can generate maximum efficiency in the omnidirectional drive mode. In Fig. 11, curve 1 is obtained by connecting the steering angles corresponding to the maximum force ratio for each robot traction force angle α_f. However, a rapid change in steering angle from +30° to -30° is required to maintain the maximum force ratio around $\alpha_f = 90^o \cdot n + 45^o (n = 0, 1, \ldots)$. Such a discontinuity in the steering angle due to a small change in traction force direction is not desirable. To overcome this problem, we employed a sinusoidal profile (curve 2).

An optimal solution that can maximize the effi-

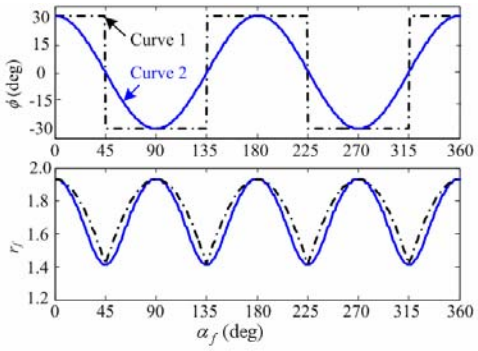

Fig. 11. Steering angle curve corresponding to the maximum force ratio as a function of robot traction force angle.

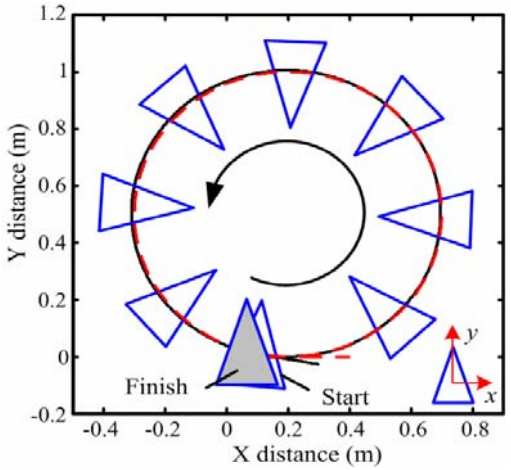

Fig. 12. Experimental results of tracking performance for a circular trajectory. (solid line: actual trajectory, dashed line: reference trajectory).

ciency of OMR-SOW may be found by considering various factors such as the operating ranges of all four motors, mechanical friction between the wheels and the surface, damping and so on. However, it is difficult (and sometimes impossible) to consider all these factors because they change constantly depending on the driving conditions. Instead, only the efficiency of a single motor was used as a criterion for the steering control algorithm in this paper. Although this algorithm cannot provide an optimal solution, it provides a simple and practical solution that is optimized for the developed mobile robot.

If the steering angle ϕ is set to either +45° or -45°as shown in Fig. 5(d), the OMR-SOW can be driven in the differential drive mode. In this mode, the OMR-SOW has the maximum force ratio denoted by A in Fig. 10, which leads to a higher efficiency than that in the omnidirectional drive mode. In conclusion, if the

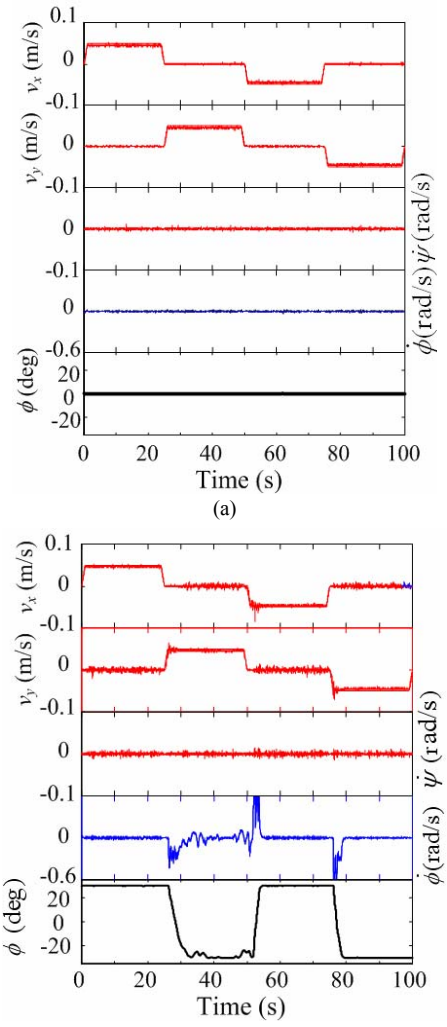

Fig. 13. Experimental results for square trajectory: (a) Fixed steering angle, and (b) Variable steering angle by steering algorithm.

CVT is controlled by considering the steering pattern for each driving condition, efficient driving can be achieved. However, the change from the omnidirectional to the differential drive mode cannot be performed while the robot is moving because a steering angle greater than ±30° usually results in a slip between the wheel and ground, and the passive rollers cannot be controlled. Hence, the robot should stop temporarily to perform this change.

4. Experiments

Various tests have been conducted to demonstrate

the performance of the constructed omnidirectional mobile robot with CVT function. Fig. 12 shows the tracking performance of OMR-SOW for a circular trajectory. This tracking was associated with both translational and rotational motion. In the experiment, the robot moved along the *x*-direction and simultaneously rotated about the *z*-axis. The actual trajectory represented by the solid line tracked the reference reasonably well. Some error was observed around the finish since the prototype vehicle did not implement any position control algorithm for this test, and thus the position error was accumulated during motion.

A series of experiments using a fixed steering angle and a steering angle computed by the proposed steering control algorithm were conducted. In Fig. 13, the robot followed a 1.5m x 1.5m square trajectory at a speed of 0.05m/s. Fig. 13(a) shows the result for a fixed steering angle and the consumed energy of 221.3J. In Fig. 13(b), the steering angle was selected according to the force direction computed for the measured currents by Eq. (12) and Fig. 10. The energy values for these experiments were measured as 179.5J. The consumed energy was reduced by 15% by the proposed steering control algorithm.

In the next experiment, a half of the square trajectory was used on a ramp with a slope of 10^{o}, as shown in Fig. 14. To follow a given velocity command, the motors should generate much more torque on a ramp than on the ground and thus the current is increased. Therefore, the measured current indirectly provides information on the ground conditions or disturbances. Even for a ramp or disturbance, the steering control algorithm based on the measured current can select the proper steering angles. The consumed energy was measured as 767.5J for the fixed angle and 653.4J for the case of the steering algorithm, indicating a 14% reduction in energy.

Next, the energy consumption was investigated based on the wheel arrangement. The robot traveled at a speed of 0.05m/s in the *y*-axis, as shown in Fig. 5. This motion could be achieved by using various wheel arrangements. Among them, four configurations were selected including three omnidirectional drive modes and one differential drive mode (see Fig. 5). The experimental results are summarized in Table 2. As expected, the differential drive provided better efficiency than the omnidirectional drives. This result justifies the proposed mechanism capable of conversion between the omnidirectional and the differential drive mode depending on the drive conditions.

Table 2. Comparison of omnidirectional drive with differential drive.

Experiments	ϕ	Average current (A)	Power (W)	Energy (J)
(a)	30	0.385	9.246	924.6
(b)	0	0.296	7.112	711.2
(c)	-30	0.275	6.605	660.5
(d)	-45	0.266	6.402	640.3

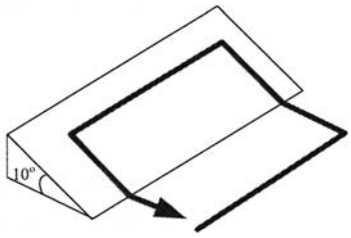

Fig. 14. Square trajectory with ramp.

The conventional wheels used in automobiles usually exhibit better performance than the omnidirectional wheels with passive rollers. This is because the height of a surmountable bump for the omnidirectional wheels is limited by the radius of the smallest passive roller and the friction force of the roller. Therefore, if the passive rollers are constrained not to rotate as in the differential drive mode, even omnidirectional wheels can function in a manner similar to conventional ones. The omnidirectional wheel can go over a 5cm high bump, which is greater than the radius of the passive roller.

5. Conclusions

An omnidirectional mobile robot with steerable omnidirectional wheels (OMR-SOW) was proposed. The structure of the robot and its kinematic analysis were presented. We developed a motion control system for the robot and conducted various experiments. From this paper, the following conclusions are drawn.

1. The OMR-SOW has 4 DOF that include 3 DOF for omnidirectional motion and 1 DOF for steering. This steering DOF functions as a continuously variable transmission (CVT). Therefore, OMR-SOW can also be considered as an omnidirectional mobile robot with CVT.
2. The proposed steering control algorithm for CVT can provide a significant reduction in driving energy than the algorithm using a fixed

steering angle. Therefore, the size of the actuator required to realize the specified performance can be reduced or the performance such as the gradability of the mobile robot can be enhanced for the given actuators.

3. The efficiency can be further improved by selecting the differential drive mode by adjusting the OMR-SOW wheel arrangement. The surmountable bump in the differential drive mode is much higher than that in the omnidirectional drive mode.

Acknowledgments

This work was supported by the Korea Science and Engineering Foundation grant (No. R11-2007-028-01002-0) and by the project of Social Security Robots funded by the Ministry of Knowledge Economy, Korea.

References

[1] K. Moore, M. Davidson, V. Bahl, S. Rich and S. Jirgal, Modeling and control of a six-wheeled autonomous robot, *Proc. of American Control Conference*, (2000) 1483-1490.

[2] J. F. Blumrich, Omnidirectional vehicle, United States Patent 3,789,947 (1974).

[3] M. West and H. Asada, Design of ball wheel mechanisms for omnidirectional vehicles with full mobility and invariant kinematics, *ASME J. of Mechanical Design*, 119 (1997) 153-161.

[4] M. Wada and S. Mori, Holonomic omnidirectional vehicles with conventional tires, *Proc. of Int. Conf. on Robotics and Automation*, (1996) 3671-3676.

[5] B. Carlisle, An omnidirectional mobile robot, Development in Robotics, Kempston, (1983).

[6] F. Pin and S. Killough, A new family of omnidirectional and holonomic wheeled platforms for mobile robot, *IEEE Trans. on Robotics and Automation*, 15 (6) (1999) 978-989.

[7] P. Muir and C. Neuman, Kinematic modeling of wheeled mobile robots, *J. of Robotic Systems*, 4 (2) (1987) 281-340.

[8] H. Asama, M. Sato, N. Goto, A. Matsumoto and I. Endo, Mutual transportation of cooperative mobile robots using forklift mechanisms, *Proc. of Int. Conf. on Robotics and Automation*, (1996) 1754-1759.

[9] M. Wada and H. Asada, Design and control of a variable footprint mechanism for holonomic omnidirectional vehicles and its application to wheelchairs, *IEEE Trans. on Robotics and Automation*, 15 (6) (1999) 978-989.

[10] J.-B. Song and K.-S. Byun, Design and control of an omnidirectional mobile robot with steerable omnidirectional wheels, *J. of Robotic Systems*, 21 (4) (2004) 193-208.

[11] S. Liu and B. Paden, A survey of today's CVT controls, *Proc. of 36th Conf. on Decision & Control*, (1997) 4738-4743.

[12] K.-S. Byun and J.-B. Song, Design and construction of continuous alternate wheels for an omnidirectional mobile robot, *J. of Robotic Systems*, 20 (9), (2003) 569-579.

[13] S. K. Saha, J. Angeles and J. Darcovich, The design of kinematically isotropic rolling robots with omnidirectional wheels, *Mechanism and Machine Theory*, 30 (8) (1995) 1127-1137.

Jae-Bok Song received the B.S. and M.S. in Mechanical Engineering from Seoul National University, Seoul, Korea, in 1983 and 1985, respectively, and the Ph.D. in Mechanical Engineering from MIT, Cambridge, MA, in 1992. Dr. Song is currently a Professor at the School of Mechanical Engineering at Korea University in Seoul, Korea. He serves as an Editor of International Journal of Control, Automation, and Systems. He is also the director at Intelligent Robotics Research Center at Korea University. His current research interests are safe manipulators, robot navigation, and design and control of the robotic systems including haptic devices and field robots.

Kyung Seok Byun received the B.S., M.S. and Ph.D. in Mechanical Engineering from Korea University in Seoul, Korea, in 1996, 1998 and 2002, respectively. Dr. Byun developed industrial robots in Mechatronics & Manufacturing Technology Center, Samsung Electronics Co., Ltd., Korea, until 2006. He is currently a Professor at the Department of Mechanical Engineering at Mokpo National University in Mokpo, Korea. His research interests are mechatronics systems and, design and control of robot system including omnidirectional mobile robot and manipulator.